AIAA 2008-4211

39th Plasmadynamics and Lasers Conference
23-26 June, Seattle, WA

"Feedforward" Adaptive-Optic Mitigation of Aero-Optic Disturbances

Alice M. Nightingale*, Benson Mitchell§, Bill Goodwine†, and Eric J. Jumper‡
Center for Flow Physics and Control
Department of Aerospace and Mechanical Engineering
University of Notre Dame, Notre Dame, IN, 46556

This paper describes a control methodology that synchronizes the deformable mirror corrections to the coherent aberrations of a regularized compressible shear layer. The controller was developed in order to automate the "feedforward" adaptive-optic control of compressible shear layer aberrations that has been successfully demonstrated in our previous efforts. Numerical simulations, in conjunction with analytical analyses, were used to select an optimal set of control parameters based on several different criteria, such as phase margin and settling time. Finally, an analog control system was constructed and tested experimentally. The results presented in this paper demonstrate the effectiveness of our alternative adaptive-optic controller in correcting for high-speed aero-optic disturbances, overcoming the bandwidth barrier confronting the conventional adaptive-optic controller.

I. Introduction

In 1953, Horace Babcock introduced the concept of Adaptive-optics (AO) [1]; a technique used to perform optical corrections by applying a conjugate waveform to the optical wavefront prior to its transmission through an aberrating medium [1]. The result is to effectively restore a planar wavefront in the ideal case. These methods have successfully corrected for low speed disturbances such as those found in atmospheric turbulence. However, in the case of high-speed aero-optic disturbances the current AO techniques become restricted due to bandwidth limitations. As the frequency content present within the aberrations increases, bandwidth limitations due to time delays, update constraints, measurement errors, response times, *etc.* become much more significant, eventually nullifying the ability to correct for the aberrations. These adverse effects become even more significant when systems with shorter wavelength lasers are used; a trend that continues to take place due to the advantages of increased far-field irradiance [2].

Aero-optic disturbances occurring near the exit aperture of an outgoing beam, such as those created in free shear layers (Figure 1), commonly exceed 1 kHz placing certain sensing and update requirements on the control system used to perform AO corrections. Each component of the AO controller has its own set of bandwidth restrictions. For example, wavefront sensors are limited by their capture rate capability, reconstructors have certain time delays associated with them, deformable mirrors (piezoelectric actuators) have certain response time characteristics, and so forth. In Ref. [3], significant bandwidth limitations were also found due to the amplifier used to power the deformable mirror. Frequency response analyses revealed that the amplifier latency alone would require capture rates that exceed current wavefront sensor technology in the case of high-speed aero-optic disturbances. Additionally, the amplifier's slew rate limitations restrict the deformable mirror's ability to perform acceptable corrections at frequencies above 1 kHz. These bandwidth limitations along with those posed by the remaining AO controller components create a need to approach the adaptive-optic problem for aero-optic disturbances in a new and innovative way.

---

* Graduate Research Assistant, Aerospace and Mechanical Engineering Department, Notre Dame, DEPS Fellow, AIAA Student Member.
§ Graduate Research Assistant, Aerospace and Mechanical Engineering Department, Notre Dame, AIAA Student Member.
† Associate Professor, Aerospace and Mechanical Engineering Department, Notre Dame.
‡ Professor, Aerospace and Mechanical Engineering Department, Notre Dame, AIAA Fellow.

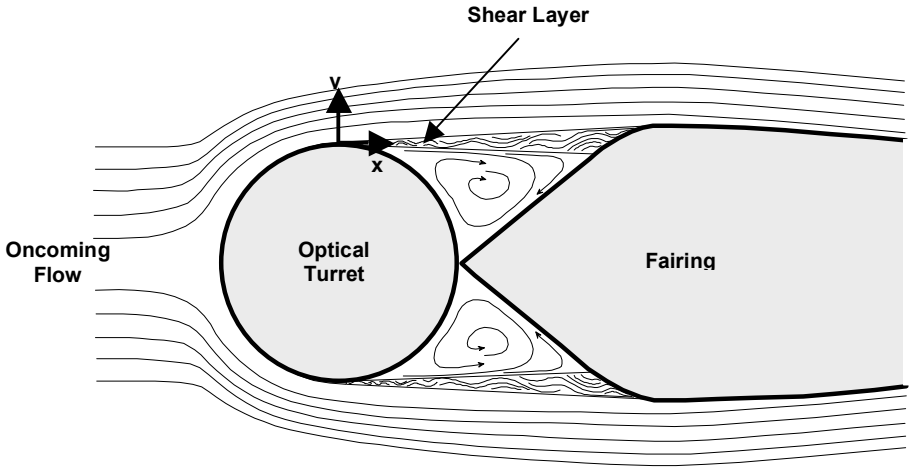

Figure 1. Shear layer formed over a turret/fairing combination.

The purpose of this paper is to report the results obtained to date on the development of an alternative AO controller, and to demonstrate it's feasibility in performing real-time corrections for high-speed aero-optic disturbances. An analog circuit has been constructed based upon the alternative AO approach proposed in Ref. [4]. This method combines flow control with a phase-lock-loop control strategy as a means of tackling the aero-optic bandwidth problem. By forcing the shear layer, a region of otherwise highly-turbulent, unpredictable flow may be regularized into more periodic and predictable large-scale structures [5][6][7]. Consequently, an estimation of the emerging optical wavefront, based on *a priori* knowledge of the forced flow, may be "fed forward" to the controller and used to perform AO corrections [8]. The waveform's amplitude and phase are controlled via a phase-lock-loop AO controller where a small aperture laser beam provides a non-intrusive means of acquiring phase and amplitude information. The following paper provides a brief description of shear layer regularization and outlines the phase-lock-loop control strategy employed. Finally, experimental results for this alternative AO controller are presented.

II. Shear Layer Regularization/Manual Correction

In Ref. [5], it was found that the large-scale structures convecting downstream in a free shear layer may be regularized by forcing the flow at or near its origin. It was shown that forcing the shear layer at its *optical natural frequency* resulted in regularization upstream from the location where the natural frequency occurs in the unforced case [5]. This in turn produces a more regular (*i.e.* more periodic) emerging optical wavefront (Fig. 2), which may be estimated as a traveling sinusoidal waveform [7]. This kind of high-speed shear layer regularization has been verified experimentally. In an experiment conducted in the University of Notre Dame's compressible shear layer facility, forcing was applied to a Mach 0.8/0.1 free shear layer using voice-coil actuators mounted to the trailing edge of the splitter plate which vibrated mechanically in a motion perpendicular to the convecting flow [6]. Regularization of the shear layer was verified by small-aperture Malley-Probe measurements which showed more regular and therefore more predictable large-scale structures [6][7]. A small aperture beam traversing through the flow transformed from an extremely unpredictable signal to maintaining a more periodic and "sinusoidal" form. Such a small aperture beam will provide a non-intrusive means of acquiring feedback information for our AO controller. The control experiments described in Section V use a function generator to simulate this "sinusoidal" jitter signal.

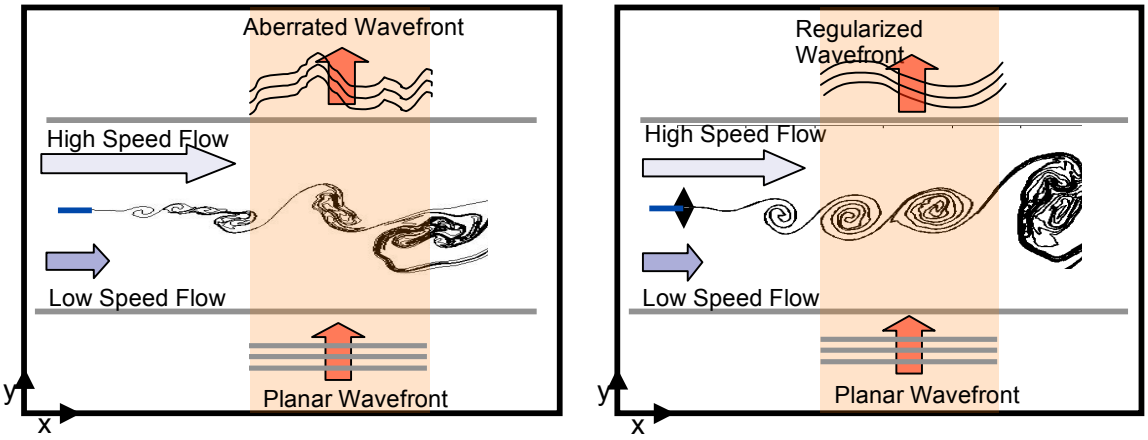

Figure 2. Irregular aberrated wavefront emerging from a high speed free shear layer (left) and a more regular, "periodic" wavefront emerging from a forced high speed free shear layer (right).

In 2006 a man-in-the-loop, high-speed, aero-optic correction was performed at Notre Dame [8]. Wavefront measurements were taken of a shear layer forced at 750 Hz. A proper-orthogonal decomposition of the wavefront data showed that the optical aberrations imposed by the forced shear layer were nearly sinusoidal in nature. The wavefront data were used to drive pre-determined deformable-mirror motions to correct the shear layer aberrations; the only requirement was that the deformable mirror motions needed to be synchronized to the regularized shear layer aberrations. For the tests detailed in Ref. [8], this synchronization took place via a man-in-the-loop approach. Wavefront measurements of the corrected beam were recorded and post-processed revealing an increase in time-averaged Strehl ratio from approximately 0.14 to 0.66, shown in Fig. 3. This successful man-in-the-loop AO correction became the basis for developing an alterative AO controller; the goal being to automate the correction procedure. This paper details the research performed in creating a real-time automatic AO controller.

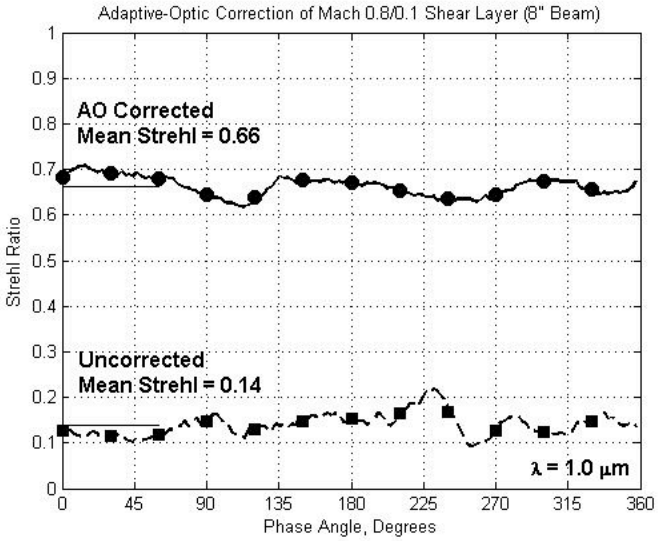

Figure 3. Post-processed Strehl ratio results for a man-in-the-loop AO correction of a Mach 0.8/0.1 shear layer performed by Dan Duffin in June of 2006 [8].

III. Alternative AO Controller

As a refinement to the feedforward AO approach described above, flow control and a phase-lock-loop controller has been proposed [4] to remove the man-in-the-loop synchronization of the deformable mirror with an automated controller. Due to the periodic nature of the regularized shear layer's emerging optical wavefront, a sinusoidal wavefront estimation is constructed by taking advantage of *a priori* flow and

forcing knowledge. The traveling conjugate correcting wavefront is applied to the deformable mirror while amplitude and phase adjustments are performed by the controller. Once the wavefronts become synchronized, the outgoing wavefront aberrations are reduced, thereby increasing the beam's on-target intensity. By assuming the regularized shear layer is dominated by a single optical frequency as shown in Ref. [7], the flow's emerging optical wavefront may be estimated as a sinusoidal wavefront with angular frequency and wave number determined from the forcing frequency and convective velocity [4]. The optical path difference (*OPD*) associated with the forced shear layer is given the assumed form,

$$OPD_{sl}(t,x) = A_{sl}\sin(k_{sl}x - \omega_{sl}t + \phi_{sl}), \tag{1}$$

where A_{sl}, k_{sl}, ω_{sl}, and ϕ_{sl} are the amplitude, wave number, angular frequency, and phase of the forced shear layer's resulting optical wavefront, respectively. Since the wave number and angular frequency of the shear layer *OPD* are known, the deformable mirror is driven by a waveform whose corresponding *OPD* is defined as

$$OPD_{DM}(t,x) = A_{DM}\sin(k_{sl}x - \omega_{sl}t + \phi_{DM}), \tag{2}$$

assuming the deformable mirror membrane can form the desired sinusoidal wave. The variables A_{DM} and ϕ_{DM} in Eq. (2) represent the amplitude and phase of the wave traveling across the deformable mirror; these two variables are unknown and optimized by the AO controller. The goal is to use estimates of A_{sl} and ϕ_{sl} to determine the amplitude, A_{DM}, and phase, ϕ_{DM}, of the deformable mirror such that $\left|OPD_{DM} - OPD_{sl}\right|$ is minimized. This is accomplished using a feedback control system known as a phase-lock-loop (PLL) [9]. The PLL uses an estimate of the phase difference between the incident wavefront and the deformable mirror to synchronize the phase of the deformable mirror's wavefront with the phase of the incident aberrated wavefront. This approach replaces the need for an array of two-dimensional real-time wavefront measurements (which become bandwidth limited in the case of high-speed aero-optic disturbances) with a single one-dimensional position sensor.

A. AO System Setup

The finalized AO system hardware will consist of a deformable mirror, two small aperture position sensing devices, a feedforward control circuit and a feedback control circuit as shown in Fig. 4. In a future high-speed shear layer experiment, a single small aperture laser beam will provide feedback information to the AO controller while a large aperture beam propagates through the flow and off the deformable mirror applying corrections. The small aperture laser beam provides a non-intrusive means of gathering feedback information for the controller. The small aperture beam will be propagated through the regularized shear layer as described in Section II. For the control experiments presented in this paper, the jitter signal from this beam is simulated using a function generator. The single beam will then be separated into two beams using a beam splitter. The incident beam will be directed onto the first position sensing device, measuring the time-varying signal due to the aberrating regularized wavefront. The signal generated by this sensor will be used as an input into the analog feedforward circuit that estimates the amplitude of the aberrated wavefront. This signal is also used in the feedback circuitry to determine the phase difference between wavefronts. The portion of the laser beam which passes through the beam splitter will be reflected off the deformable mirror and redirected by the beam splitter onto another position sensing device producing a signal equivalent to the shear layer jitter minus the deformable mirror jitter (θ_{sl} - θ_{DM}). This signal will be subtracted from the shear layer jitter signal to recover the jitter associated with the deformable mirror alone.

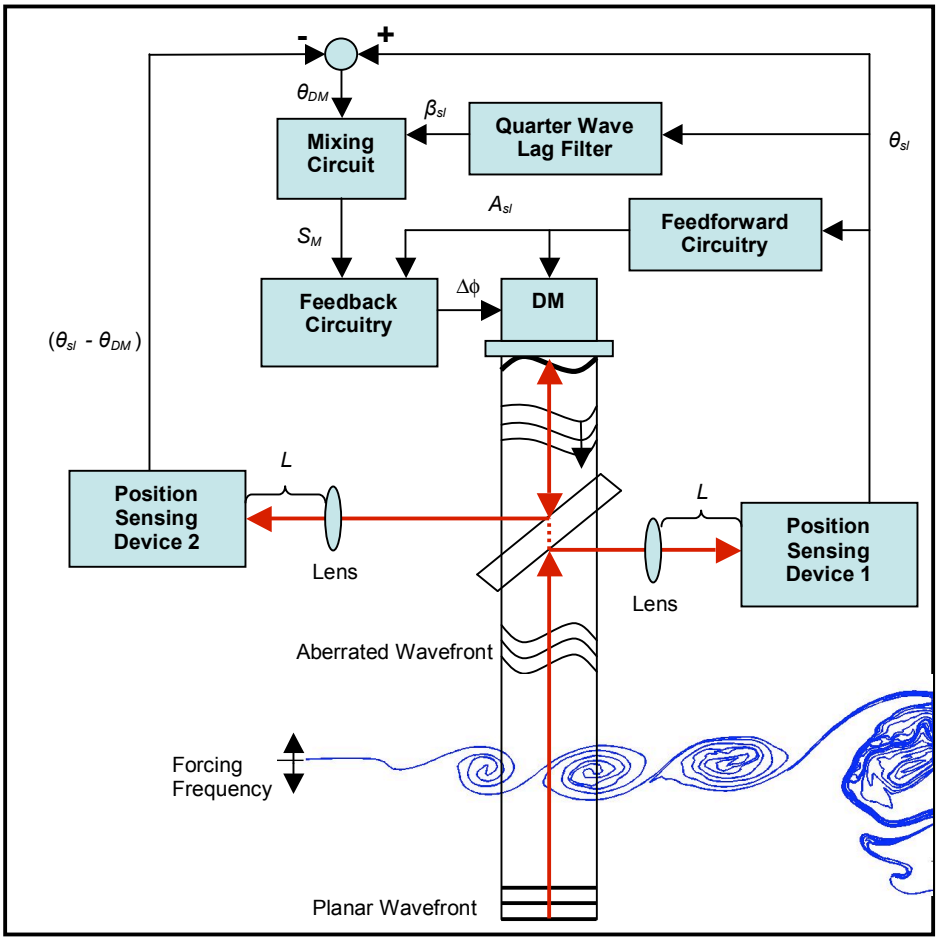

Figure 4. Adaptive-Optic controller and high-speed shear layer experimental setup.

B. Phase-Lock-Loops (PLLs)

Phase-lock-loops (PLLs) are one of the most common feedback systems designed and built by engineers. They are used in a variety of applications such as communication and storage devices, radio and television, etc. A PLL adjusts its frequency with the goal of synchronizing itself with a reference source or input signal. The typical PLL consists of a phase detector (PD), loop filter (LF), and voltage-controlled oscillator (VCO). The PD compares the phase of the reference source with the output from the VCO; this may be accomplished using a multiplier (or mixer) along with a low pass filter. The reference source is mixed, or multiplied, with the output signal producing both a sum and a difference signal. When the frequency becomes locked, this results in a harmonic term at twice the input frequency and a D.C. bias term. A low pass filter is used to attenuate the double frequency term, yielding a D.C. error signal proportional to the phase difference between the reference source and the VCO output. The LF filters the error signal and provides a useful design tool for the control engineer to create the desired system tracking response. Second and third order closed loop transfer functions are commonly designed due to their stability and tracking characteristics. Figure 5 shows a block diagram of a typical PLL. The PD is represented by the mixing block and low pass filter combination.

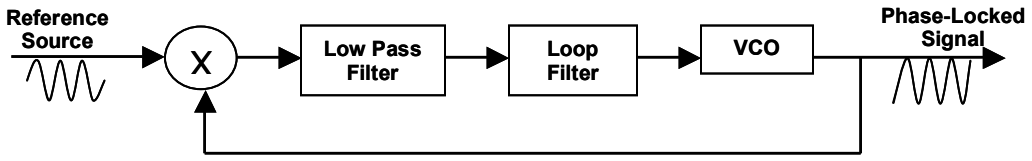

Figure 5. Block diagram of a typical PLL.

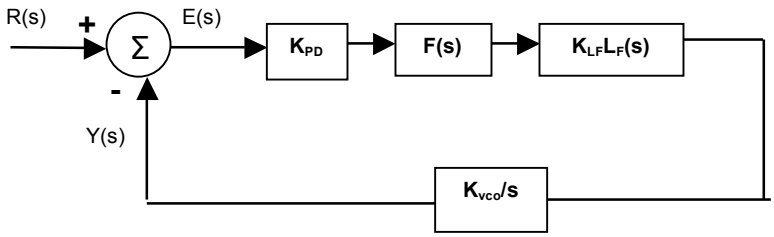

Figure 6. Block diagram of a conceptual PLL model.

In order to apply linear control techniques to the PLL a more conceptual model must be used. Figure 6 shows the block diagram for the linearized PLL model. A summation block is used to represent the mixing function of the PD. The output signal (phase-locking signal), *Y(s)*, is subtracted from the reference phase signal, *R(s)*, generating an error signal, *E(s)*. The error is then scaled by K_{PD}, representing the gain magnitude of the phase detector and passed through the low pass filter, *F(s)*. The loop function, $L_F(s)$, performs any other necessary filtering action while maintaining closed loop system stability. Finally, the VCO acts as an integrator, where K_{VCO} represents the sensitivity constant of the device. The closed loop transfer function for the system shown in Fig. 6 is

$$T(s) = \frac{Y(s)}{R(s)} = \frac{K_{PD}K_{LF}K_{VCO}F(s)L_F(s)}{s + K_{PD}K_{LF}K_{VCO}F(s)L_F(s)}, \tag{3}$$

where *F(s)* represents the low pass filter and $L_F(s)$ the loop filter function designed by the engineer to meet desired response characteristics. In order to design a system with zero tracking error for both a step input and a ramp input, the closed loop transfer function must contain two poles at zero (one of which is typically obtained with the VCO) in addition to the low pass filter's left half plane pole. A minimum phase zero must also be included to maintain closed-loop system stability. Section IV describes the control system analysis performed in selecting the low pass filter and loop filter parameters.

C. Analog Control Circuit Components

The analog control circuit consists of a PLL controller, a feedforward amplitude estimator, and a series of phase-lag circuits that produce six additional signals that are incrementally phase shifted from the original phase-locked signal. These seven signals will be used to control the seven rows of actuators creating the desired spatial waveform traveling across the deformable mirror. Figure 7 shows a picture of the AO controller's circuitry. The following section describes the method of selecting the control parameters based on certain design criteria.

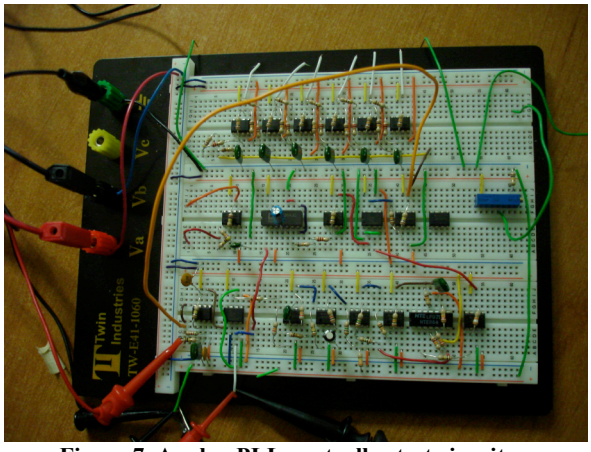

Figure 7. Analog PLL controller test circuitry.

IV. Phase-Lock-Loop Analysis

A PLL control strategy was designed with the goal of synchronizing the deformable mirror's conjugate correction with the regularized wavefront emerging from a forced shear layer. As shown in Fig. 4, the jitter signal from a small-aperture beam projected through the flow acts as the PLL's reference source used for phase-locking. The response characteristics of the phase-locking process is dependant upon the control parameters used in the control system. A set of design criteria was chosen to aid in the selection of these parameter values. Phase margin, settling time, and the integral of time multiplied by absolute error (ITAE) served as metrics when analyzing the response of the PLL controller.

The two PLL components with design flexibility are the low pass filter and the loop filter; the low pass filter is modeled based upon the expected reference frequency while the loop filter is designed with specific closed-loop response characteristics in mind. In order to achieve an asymptotic response with zero tracking error to both step and ramp changes in phase a second order PLL must be employed; a double integrator enables the circuit to track step and ramp changes in phase while a minimum phase zero ensures closed-loop system stability. Therefore, the low pass filter and loop filter Laplace transforms are given by,

$$F(s) = \frac{\omega_p}{s + \omega_p} \tag{4}$$

and

$$L_F(s) = \frac{K_{LF}(s + \omega_z)}{s\omega_z}, \tag{5}$$

respectively. Recall that the Laplace transform representing the VCO is given by

$$V(s) = \frac{K_{VCO}}{s}, \tag{6}$$

resulting in an open-loop transfer function,

$$GH(s) = \frac{K_{PD}K_{LF}K_{VCO}(s/\omega_z + 1)}{s^2 + [(1/\omega_p)s + 1]} \tag{7}$$

and a closed-loop transfer function,

$$T(s) = \frac{K_{PD}K_{LF}K_{VCO}(s/\omega_z + 1)}{1/\omega_p\, s^3 + s^2 + K_{PD}K_{LF}K_{VCO}(1/\omega_z)s + K_{PD}K_{LF}K_{VCO}} \tag{8}$$

derived from Eqn. (3). To simplify the analysis, the open-loop system's pole and zero are assumed to be above and below the unity gain bandwidth (ω_u) by a factor of δ, respectively where

$$\delta = \frac{\omega_u}{\omega_z} = \frac{\omega_p}{\omega_u}. \tag{9}$$

Upon substituting Eqns. (9) into Eqn. (7), the relationship shown in Fig. 8 is obtained where the phase margin is a function of δ: PM(δ). Phase margin is a metric commonly used to quantify system stability; a larger positive value of phase margin is most desirable. It is clear from the plot that as δ increases, the phase margin asymptotically approaches 90 degrees; therefore increasing the value of δ beyond approximately fifteen no longer becomes significantly advantageous.

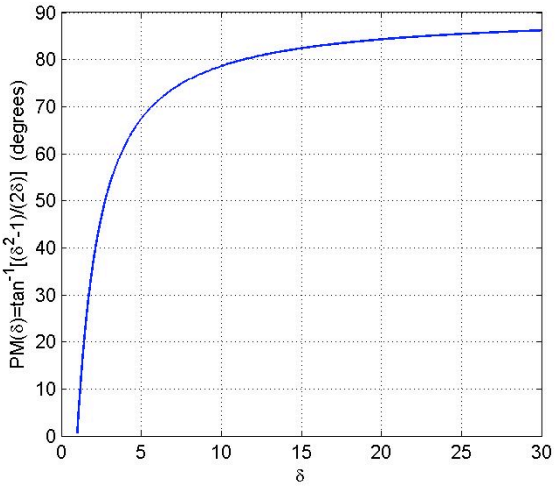

Figure 8. Phase margin as a function of the pole placement factor above the unity gain bandwidth, δ.

The second metric used to analyze the PLL controller was settling time (T_s), defined as the time required for the system's output to remain within a certain percentage of the desired response [10]. Step and ramp response functions were derived from the closed-loop transfer function given in Eqn. (8). Figure 9 shows settling times for a step response (left) and ramp response (right) versus δ for a given set of pole placement values.

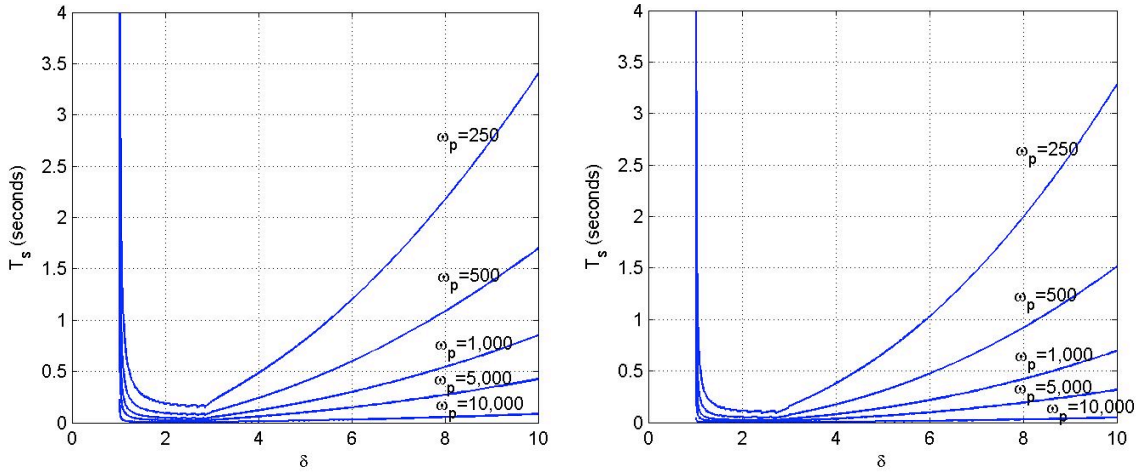

Figure 9. Settling time versus δ (the pole placement factor above the unity gain bandwidth) for various pole locations given a step (left) and a ramp (right) phase response.

Finally, the ITAE performance index was also used as a metric to analyze the control system. This criterion provides a useful measure of the performance based on the system's error accumulated over time [10]. Figure 10 shows the ITAE performance index plotted as a function of δ. Recall that the low pass filter design is based upon the expected operating frequency (750 Hz for the experiments documented in this paper). This filtering condition along with the three design metrics shown in Figs. 8, 9, and 10 were used to determine an optimal set of PLL parameters. The controller was designed with a value of approximately 2.35 for the factor δ and 200 for the pole placement, ω_p, corresponding to a low pass filter cutoff frequency of approximately 80 Hz.

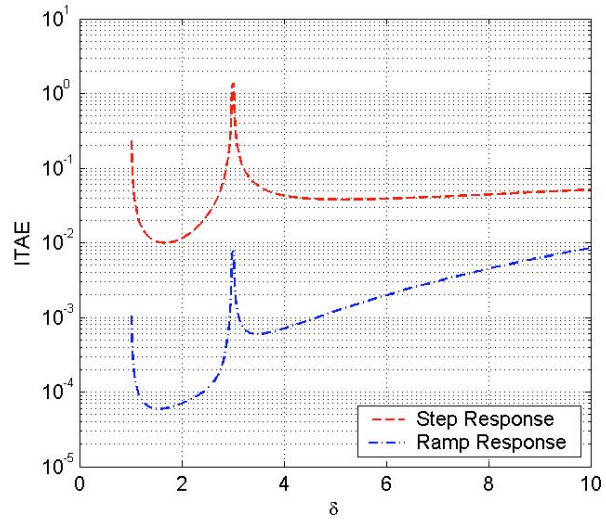

Figure 10. ITAE performance criterion plotted versus δ (the pole placement factor above the unity gain bandwidth) given a step and a ramp phase response.

The finalized PLL design was then modeled in Matlab and used to simulate the control system response. A discrete vortex method and Weakly Compressible Model [11] were used to simulate a forced shear layer and its emerging optical wavefront. Figure 11 shows the phase response along with the calculated Strehl ratio as a function of time for the numerically simulated AO PLL correction. Finally, the analog PLL controller was constructed by selecting resistor and capacitor values based upon this design analysis. The following section presents experimental results for this alternative AO controller.

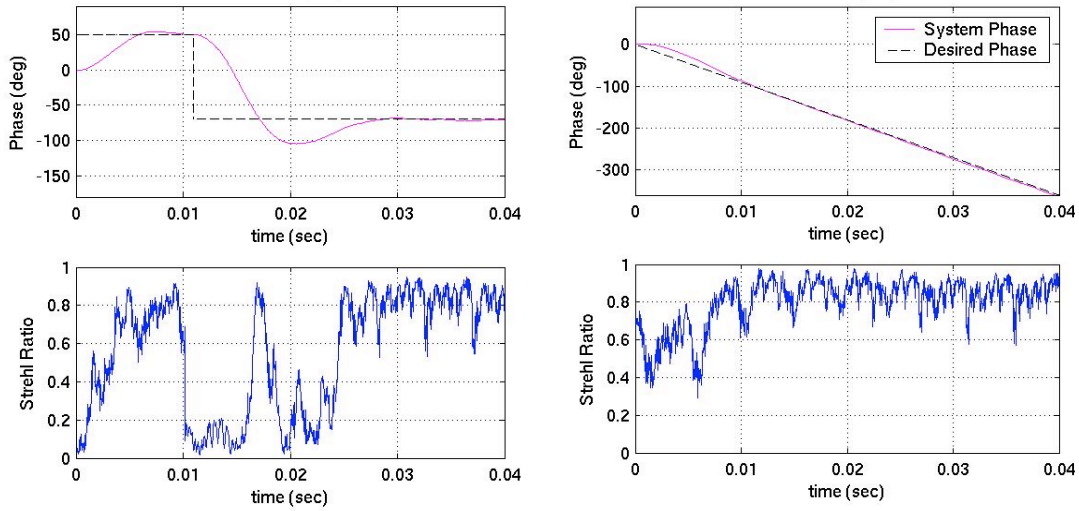

Figure 11. Phase-locking response of the simulated PLL controller and the corresponding calculated Strehl ratio for a AO correction given a step change in phase (left) and a ramp change in phase (right) between the correcting wavefront and the shear layer's aberrating wavefront.

V. Experimental Results

The PLL AO controller described heretofore was tested experimentally using a function generator as a reference source. The controller was designed to operate optimally given a 750 Hz shear layer jitter signal, corresponding to the man-in-the-loop experiment. Therefore, a 750 Hz function generator signal was input into the controller, simulating the jitter signal that will be measured via a small aperture position sensing device in the final alternative AO control demonstration. Upon powering the PLL controller, a sinusoidal signal was generated phase-locking to the reference source within seconds. The amplitude of the phase-locked signal also adjusted to match the reference.

Several different experiments were conducted to test the PLL's response characteristics including its amplitude and phase response. Figure 12 shows amplitude error as a function of the time from when the controller was first turned on. It is clear from Fig. 12 that the amplitude of the phase-locking signal asymptotically approaches the reference amplitude, maintaining less than approximately 1 % error within 0.25 seconds. Several more experiments were run in which similar results were obtained. The amplitude of the reference signal was also varied during several tests to ensure the controllers ability to track amplitude variations.

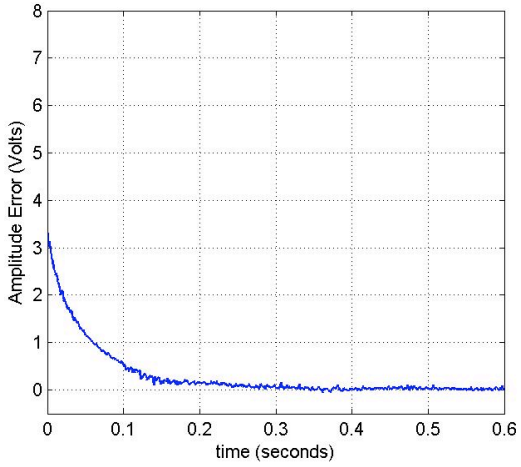

Figure 12. Experimental amplitude error versus time elapsed once PLL controller is turned on given a 750 Hz reference signal with amplitude of 8 Volts.

Additionally, the phase response of the PLL controller was studied. Figure 13 shows the phase error as a function of time for a given test. The controller was able to phase-lock with the reference signal within approximately 1.5 seconds. Several more tests were run demonstrating similar results. The ability of the controller to track step and ramp changes in phase was studied by varying the reference signals phase accordingly during the test. The PLL was able to readjust its frequency and regain phase-locking with the reference source in each case, providing frequency jumps of approximately 10 Hz and less. Further refinement to the PLL circuit will be conducted with the goal of reducing the oscillatory response (increase dampening) and decreasing settling time.

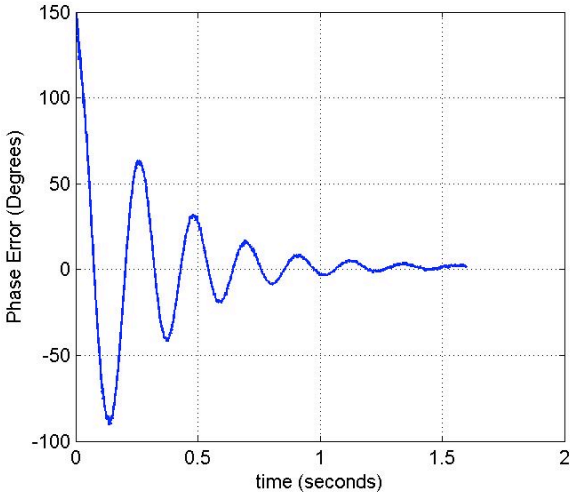

Figure 13. Experimental phase error versus time elapsed once PLL controller is turned on given a 750 Hz reference signal with amplitude of 8 Volts.

The analog controller also contains six phase lag circuits which apply consecutive phase shifts to the original phase-locked signal. The resulting seven signals with equally spaced phase shifts are used to

construct a two-dimensional traveling waveform. Figure 14 shows three consecutive wavefronts generated from these phase-shifted signals.

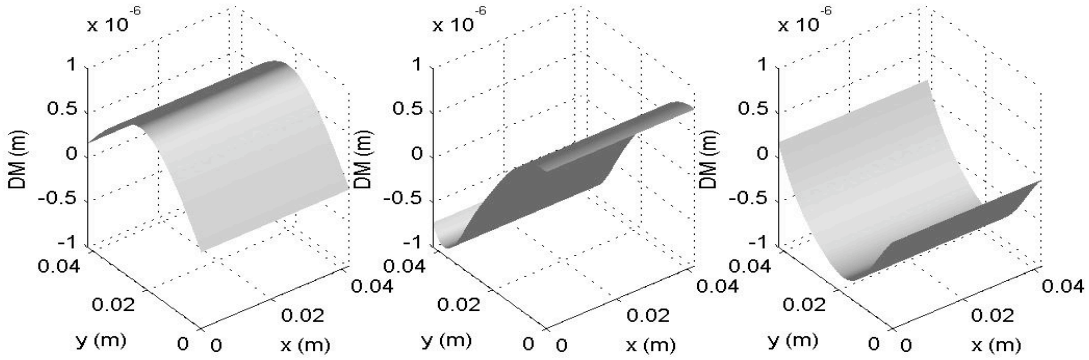

Figure 14. Two-dimensional wavefronts created from the PLLs seven phase-shifted signals (these signals will be used to control the deformable mirror used to perform AO corrections).

A traveling wavefront such as the one depicted above in Fig. 14 will be used to apply conjugate corrections to a large aperture laser beam traversing through the high-speed forced shear layer. The seven signals will control each of the seven rows of actuators used to manipulate the deformable mirror shown in Fig. 15.

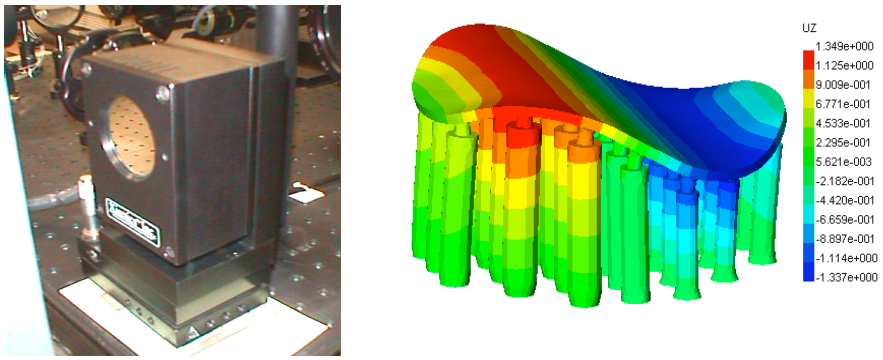

Figure 15. Xinetics DM photograph (left) and 3-D model of mirror and actuators (right).

VI. Conclusions

Due to the high-frequency nature of aero-optic disturbances, conventional AO systems are bandwidth limited in their correction capability. An alternative approach has been proposed in which flow control is combined with a PLL control strategy. This method reduces the amount of feedback information necessary to perform corrections by replacing the bandwidth-limited wavefront sensor with two small aperture position sensing devices. Forcing the shear layer at its origin creates a region of more regular large-scale structures and subsequently a more periodic optical wavefront. The "periodic" nature of this emerging optical wavefront provides *a priori* knowledge which may be taken advantage of in a "feedforward" control scheme. A PLL controller is used to lock the AO correction with the aberrating wavefront while amplitude adjustments occur simultaneously. Three design metrics were used to evaluate system performance and select an optimal set of PLL parameters; phase margin provided a measure of system stability, while settling time and ITAE criterion quantified the system's response characteristics. After performing the control analysis, an analog PLL controller was constructed and tested. Experimental results demonstrated the controller's amplitude and phase-locking adjustment capabilities. The success of Notre Dame's man-in-the-loop aero-optic correction experiment in combination with the phase-locking results presented here for the alternative AO controller offer a significant breakthrough in overcoming the aero-optic bandwidth problem. Work is currently being done to connect the PLL AO controller described in this paper to Notre Dame's deformable mirror. A future experiment is scheduled to demonstrate an automated AO correction of a high-speed shear layer using this controller.

Acknowledgements

These efforts were sponsored by the Air Force Office of Scientific Research, Air Force Materiel Command, USAF, under Grant Number FA9550-06-1-0160. The U.S. Government is authorized to reproduce and distribute reprints for governmental purposes notwithstanding any copyright notation thereon. The authors are also grateful to the Directed Energy Professional Society for its support as well as the invaluable instruction and guidance offered by Dr. Michael Lemmon of Notre Dame's Electrical Engineering Department.

References

[1] Tyson, R.K., *Principles of Adaptive Optics*, 2nd ed., Academic Press, Chestnut Hill Massachusetts, 1991.

[2] Jumper, E.J., and E.J. Fitzgerald, "Recent Advances in Aero-Optics", *Progress in Aerospace Sciences*, **37**, 2001, pp.299-339.

[3] Nightingale, A. *et al.*, "'Feedforward' Adaptive-Optic System Identification Analysis for Mitigating Aero-Optic Disturbances," *AIAA Paper 2007-4013*, Miami, June, 2007.

[4] Nightingale, A. *et al.*, "Adaptive-Optic Correction of a Regularized Weakly-Compressible Shear Layer," *AIAA Paper 2006-3072*, San Francisco, June, 2006.

[5] Nightingale, A. *et al.*, "Regularizing Shear Layer for Adaptive Optics Control Application," *AIAA Paper 2005-4774*, Toronto, June, 2005.

[6] Rennie, R. M., Siegenthaler, J. P., and Jumper, E. J., "Forcing of a Two-Dimensional, Weakly-Compressible Subsonic Free Shear Layer", *AIAA 2006-0561*, Reno, Jan. 2006.

[7] Rennie, R. M., Duffin, D. A., and Jumper, E. J., "Characterization of a Forced Two-Dimensional, Weakly-Compressible Subsonic Free Shear Layer," *AIAA 2007-4007*, June, 2007.

[8] Duffin, D. A., "Feedforward Adaptive-Optic Correction of a Weakly-Compressible High Subsonic Shear Layer," Ph.D. Dissertation, Dept. of Aerospace and Mechanical Engineering, Univ. of Notre Dame, Notre Dame, IN, 2008.

[9] Ziemer, R.E. and Peterson R.L., *Digital Communications and Spread Spectrum Systems*, MacMillan Publishing Co., New York, 1985.

[10] Dorf, R. C., and Bishop, R. H., *Modern Control Systems: Ninth Edition*, Prentice Hall, Inc., New Jersey, 2001.

[11] Fitzgerald, E. J. and Jumper E.J., "The Optical Distortion Mechanism in a Nearly Incompressible Free Shear Layer," *Journal of Fluid Mechanics*, **512**, 2004, pp. 153-189.